SPEEDAM 2008
International Symposium on Power Electronics,
Electrical Drives, Automation and Motion

Space Vector Modulation of a Six-Phase VSI based on three-phase decomposition

Gabriele Grandi, Giovanni Serra, Angelo Tani

Dept. of Electrical Engineering, University of Bologna
Viale Risorgimento, 2 – 40136 Bologna (IT)

***Abstract*—A new space vector modulation (SVM) technique having a full and independent control of the multiple voltage space vectors of a six-phase voltage source inverter is presented in this paper. The proposed space vector approach is based on three-phase decomposition, leading to the modulation of two three-phase VSIs. The six-phase load consists in a dual three-phase induction motor, with insulated neutral points. The voltage limits are investigated and the analytical developments are proved by a complete set of simulation results.**

***Index Terms*—Dual three-phase motors, multiple space vectors, space vector modulation, three-phase decomposition.**

I. Introduction

Multi-phase motor drives have many advantages over the traditional three-phase motor drives such as reducing the amplitude and increasing the frequency of torque pulsations, reducing the rotor harmonic current losses and lowering the dc link current harmonics. In addition, owing to their redundant structure, multi-phase motor drives improve the system reliability. As a consequence, the use of multi-phase inverters together with multi-phase ac machines has been recognized as a viable approach to obtain high power ratings with current limited devices [1]-[2].

The dual three-phase induction machine is undoubtedly the most frequently considered multiphase machine for high power applications. Its asymmetrical stator winding configuration is obtained with two sets of three-phase windings, spatially shifted by 30 electrical degrees, whereas the rotor winding is of squirrel cage type. In this case, the rated current of one switch of the six-phase VSI is halved compared to a three-phase drive of the same power and phase voltage rating.

This machine offers some further advantages, such as the possibility to build the six-phase inverter as a hardware combination of two standard three-phase VSIs, having proved reliability and effective protection circuitry. Furthermore, the stator core laminations of the ac machine have a number of slots multiple of three, offering the possibility to realize the multi-phase stator core with minimum adjustment with respect to standard three-phase machines.

A useful mathematical model of a dual three-phase induction machine can be obtained introducing a multiple space vector representation, called "vector space decomposition" (VSD) [3]. In particular, the behavior of the machine can be described in terms of two independent space vectors, moving arbitrarily in different d-q planes, called d_1-q_1 and d_5-q_5 in this paper.

In order to fully exploit the potentialities of the dual three-phase machine, an opportune modulation strategy for the six-phase VSI, able to independently control the two stator voltage space vectors, has to be developed. This feature is crucial in the case of a single six-phase VSI feeding two series-connected dual three-phase induction machines [4].

Nowadays, the modulation of six-phase VSIs has been widely discussed in [3]-[9]. However, a space vector modulation (SVM) algorithm for six-phase VSIs able to arbitrarily regulate both the two multiple voltage space vectors has not been presented yet.

In particular, in [3] a SVM technique based on the VSD has been proposed, with reference to the modulation of the voltage space vector on d_1-q_1, being null the voltage space vector on d_5-q_5. This SVM technique has been further developed in [5], [6] in order to reduce the stator current ripple. The implementation of the resulting modulation techniques is quite complex.

A different approach has been discussed in [7]-[9], where a simplified three-phase decomposition is considered, taking into account only the d_1-q_1 voltage space vector.

A novel SVM approach based on complete three-phase decomposition is presented in this paper. The proposed method allows a full and independent control of both the voltage space vectors on d_1-q_1 and d_5-q_5 planes, with an optimal exploitation of the dc input voltage. A similar approach has been introduced in [10] for a nine-phase VSI. The effectiveness of the proposed method has been verified by a complete set of numerical tests, carried out by introducing the model of a dual three-phase induction machine.

II. Space Vector Transformations for Six-Phase Systems

A. Multiple Space Vector Transformation

A possible space vector transformation for an asymmetric six-phase system leads to the following three space vectors [3],

978-1-4244-1664-6/08/$25.00 ©2008 IEEE

$$\bar{x}_h = \frac{1}{3}\left[x_1 + x_2\alpha^h + x_3\alpha^{4h} + x_4\alpha^{5h} + x_5\alpha^{8h} + x_6\alpha^{9h} \right], \quad (1)$$

being $\alpha = exp\ (j\pi/6)$, and h = 1, 3, 5. By developing (1) with respect to the index h yields

$$\begin{cases} \bar{x}_1 = \frac{1}{3}\left[x_1 + x_2\alpha + x_3\alpha^4 + x_4\alpha^5 + x_5\alpha^8 + x_6\alpha^9 \right] \\ \bar{x}_3 = \frac{1}{3}\left[(x_1 + x_3 + x_5) + j(x_2 + x_4 + x_6) \right] \\ \bar{x}_5 = \frac{1}{3}\left[x_1 + x_2\alpha^5 + x_3\alpha^8 + x_4\alpha + x_5\alpha^4 + x_6\alpha^9 \right] \end{cases}. \quad (2)$$

Note that the space vector $\bar{x}_3$ has a singular expression since 3 is a factor of the number of phases n = 6, which is not a prime. The inverse transformation of (2) is

$$\begin{cases} x_1 = \bar{x}_3 \cdot 1 + \left(\bar{x}_1 + \bar{x}_5^*\right) \cdot 1 \\ x_2 = \bar{x}_3 \cdot j + \left(\bar{x}_1 - \bar{x}_5^*\right) \cdot \alpha \\ x_3 = \bar{x}_3 \cdot 1 + \left(\bar{x}_1 + \bar{x}_5^*\right) \cdot \alpha^4 \\ x_4 = \bar{x}_3 \cdot j + \left(\bar{x}_1 - \bar{x}_5^*\right) \cdot \alpha^5 \\ x_5 = \bar{x}_3 \cdot 1 + \left(\bar{x}_1 + \bar{x}_5^*\right) \cdot \alpha^8 \\ x_6 = \bar{x}_3 \cdot j + \left(\bar{x}_1 - \bar{x}_5^*\right) \cdot \alpha^9 \end{cases}, \quad (3)$$

where symbols " · " and " * " denote inner (scalar) product and complex conjugate, respectively. The three space vectors $\bar{x}_1$, $\bar{x}_3$, and $\bar{x}_5$ lie in the planes called d_1-q_1, d_3-q_3, and d_5-q_5, respectively.

B. Three-Phase Space Vector Decomposition

The six-phase system can be seen as the composition of two three-phase sub-systems {1} and {2} according to

$$\{1\}\begin{cases} x_1^{(1)} = x_1 \\ x_2^{(1)} = x_3 \\ x_3^{(1)} = x_5 \end{cases} \quad \{2\}\begin{cases} x_1^{(2)} = x_2 \\ x_2^{(2)} = x_4 \\ x_3^{(2)} = x_6 \end{cases}. \quad (4)$$

The space vectors $\bar{x}^{(1)}$, $\bar{x}^{(2)}$ and the zero-sequence components $x_0^{(1)}$, $x_0^{(2)}$ can be defined for each sub-system {1}, {2}, leading to

$$\begin{cases} \bar{x}^{(1)} = \frac{2}{3}\left[x_1^{(1)} + x_2^{(1)}\alpha^4 + x_3^{(1)}\alpha^8 \right] \\ x_0^{(1)} = \frac{1}{3}\left[x_1^{(1)} + x_2^{(1)} + x_3^{(1)} \right] \end{cases} \quad \begin{cases} \bar{x}^{(2)} = \frac{2}{3}\left[x_1^{(2)} + x_2^{(2)}\alpha^4 + x_3^{(2)}\alpha^8 \right] \\ x_0^{(2)} = \frac{1}{3}\left[x_1^{(2)} + x_2^{(2)} + x_3^{(2)} \right] \end{cases}. \quad (5)$$

The relationships between the multiple space vectors of the six-phase system and the two space vectors of the three-phase sub-systems are obtained by introducing (4) and (5) in (1), leading to

$$\begin{cases} \bar{x}_1 = \frac{1}{2}\left[\bar{x}^{(1)} + \alpha\, \bar{x}^{(2)} \right] \\ \bar{x}_3 = x_0^{(1)} + j x_0^{(2)} \\ \bar{x}_5^* = \frac{1}{2}\left[\bar{x}^{(1)} - \alpha\, \bar{x}^{(2)} \right] \end{cases}. \quad (6)$$

The space vectors $\bar{x}^{(1)}$, $\bar{x}^{(2)}$ and the zero-sequence components $x_0^{(1)}$, $x_0^{(2)}$ of the three-phase sub-systems can be expressed on the basis of the multiple space vectors $\bar{x}_1$, $\bar{x}_5^*$, and $\bar{x}_3$ as

$$\begin{cases} \bar{x}^{(1)} = \bar{x}_1 + \bar{x}_5^* \\ x_0^{(1)} = \bar{x}_3 \cdot 1 \end{cases}, \quad \begin{cases} \bar{x}^{(2)} = \alpha^{-1}\left(\bar{x}_1 - \bar{x}_5^*\right) \\ x_0^{(2)} = \bar{x}_3 \cdot j \end{cases}. \quad (7)$$

III. Six-Phase VSI Feeding a Load with Insulated Neutral Points

The scheme of a six-phase VSI feeding a balanced load connected as a double three-phase system having insulated neutral points $0^{(1)}$, $0^{(2)}$ is represented in Fig. 1.

As shown in Fig. 1 and expressed by (4), the six load voltages v_1, v_2, …, v_6 can be seen as the combination of the three voltages $v_1^{(h)}$, $v_2^{(h)}$, $v_3^{(h)}$ of the two three-phase sub-systems $h = \{1\},\{2\}$. In the same way, the six-phase inverter can be seen as the combination of two standard three-phase VSIs connected to the same dc bus.

A. Multiple Space Vectors of the Load Voltages

By applying (2) to load voltages, yields $v_0^{(1)} = v_0^{(2)} = 0$ and $\bar{v}_3 = 0$, being the neutral points insulated. The remaining space vectors can be written as

$$\begin{cases} \bar{v}_1 = \frac{1}{3}V_{dc}\left[S_1 + S_2\alpha + S_3\alpha^4 + S_4\alpha^5 + S_5\alpha^8 + S_6\alpha^9 \right] \\ \bar{v}_5 = \frac{1}{3}V_{dc}\left[S_1 + S_2\alpha^5 + S_3\alpha^8 + S_4\alpha + S_5\alpha^4 + S_6\alpha^9 \right] \end{cases}. \quad (8)$$

There are 2^6 = 64 possible switch configurations. For space vectors 1 and 5, (i.e., in d_1-q_1 and d_5-q_5 planes), there are four configurations corresponding to the null voltage vector, i.e, (000000), (111111), (101010), and

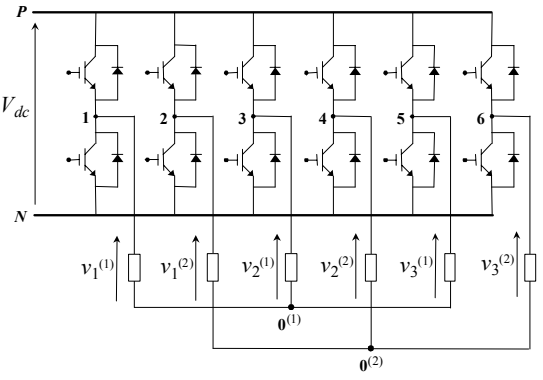

Fig. 1. Scheme of a six-phase VSI feeding a six-phase load with insulated neutral points.

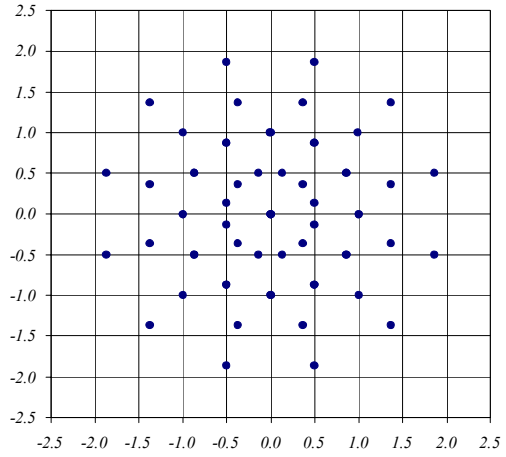

Fig. 2. Normalized voltage space vectors (with respect to 1/3 V_{dc}) of the six-phase VSI on d_1-q_1 and d_5-q_5 planes.

(010101). The remaining 60 active configurations are represented by 48 different voltage vectors in each *d-q* plane, as depicted in Fig. 2.

B. Space Vector Modulation

As stated above, the case of insulated neutral points, leads to $v_0^{(1)} = v_0^{(2)} = 0$, whereas the space vector component of the load voltages can be written on the basis of (5) as

$$\begin{cases} \overline{v}^{(1)} = \dfrac{2}{3} V_{dc} \left[S_1^{(1)} + S_2^{(1)} \alpha^3 + S_3^{(1)} \alpha^6 \right] \\ \overline{v}^{(2)} = \dfrac{2}{3} V_{dc} \left[S_1^{(2)} + S_2^{(2)} \alpha^3 + S_3^{(2)} \alpha^6 \right] \end{cases} . \tag{9}$$

The space vectors $\overline{v}^{(1)}$ and $\overline{v}^{(2)}$ correspond to the output voltage space vectors of standard three-phase VSIs, as represented in Fig. 3. By combining (9) with (6) it is possible to determine the number of active voltage vectors as $7^2 - 1 = 48$, as stated in the previous sub-section.

The input variables for the SVM of the six-phase VSI are usually represented by multiple voltage space vector references, $\overline{v}_{1ref}$ and $\overline{v}_{5ref}$. The method proposed in this paper consists in determining the reference voltage space vector for the two three-phase VSIs by applying (7), leading to

$$\begin{cases} \overline{v}_{ref}^{(1)} = \overline{v}_{1ref} + \overline{v}_{5ref}^{*} \\ \overline{v}_{ref}^{(2)} = \alpha^{-1} \left(\overline{v}_{1ref} - \overline{v}_{5ref}^{*} \right) \end{cases} . \tag{10}$$

The space vectors determined in (10) can be independently synthesized by using the well-know three-phase SVM technique, as represented in Fig. 3. It should be noted that (10) allows the extension of the modulation proposed in [7]-[9] to the case of $\overline{v}_{5ref} \neq 0$.

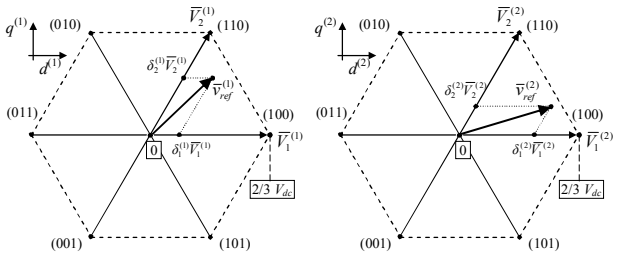

Fig. 3. Output voltage space vectors for the two three-phase VSIs.

Then, duty-cycles $\delta_1^{(h)}$ and $\delta_2^{(h)}$ of the adjacent vectors $\overline{V}_1^{(h)}$ and $\overline{V}_2^{(h)}$ for the three-phase VSIs (h = 1, 2) are calculated by the following relationships:

$$\begin{cases} \delta_1^{(h)} = \dfrac{\overline{v}_{ref}^{(h)} \cdot j\overline{V}_2^{(h)}}{\overline{V}_1^{(h)} \cdot j\overline{V}_2^{(h)}} \\ \delta_2^{(h)} = \dfrac{\overline{v}_{ref}^{(h)} \cdot j\overline{V}_1^{(h)}}{\overline{V}_2^{(h)} \cdot j\overline{V}_1^{(h)}} \end{cases} , \quad h = 1, 2. \tag{11}$$

Duty-cycles $\delta_0^{(h)}$ and $\delta_3^{(h)}$ of the null configurations (000) and (111) are determined to complete the switching period, according to

$$\delta_0^{(h)} + \delta_3^{(h)} = 1 - (\delta_1^{(h)} + \delta_2^{(h)}), \quad h = 1, 2. \tag{12}$$

Time-sharing between null configurations is arbitrary, as for a standard three-phase VSI, leading to two degrees of freedom in the modulation process. These degrees of freedom could be exploited to minimize the current ripple and/or to handle the switching frequency by introducing continuous or discontinuous switching modes [6]. In particular, for each three-phase VSI, the condition $\{\delta_0^{(h)} \neq 0$ and $\delta_3^{(h)} \neq 0\}$ corresponds to a continuous switching mode, whereas the condition $\{\delta_0^{(h)} = 0$ or $\delta_3^{(h)} = 0\}$ correspond to a discontinuous switching mode, leading to 9 different switching modes for the whole six-phase VSI. "Symmetrical" SVM operation can be obtained for both three-phase VSI by considering $\delta_0^{(1)} = \delta_3^{(1)}$ and $\delta_0^{(2)} = \delta_3^{(2)}$.

C. Voltage Limits

The voltage limit is determined for the voltage space vector $\overline{v}_{1ref}$, with reference to the condition: $\overline{v}_{3ref} = 0$, $\overline{v}_{5ref} = 0$, as in the case of sinusoidal balanced voltages. In this case, (10) leads to the following voltage space vectors $\overline{v}_{ref}^{(h)}$ for the two three-phase VSIs:

$$\begin{cases} \overline{v}_{ref}^{(1)} = \overline{v}_{1ref} \\ \overline{v}_{ref}^{(2)} = \alpha^{-1} \overline{v}_{1ref} \end{cases} . \tag{13}$$

Being the two three-phase VSIs independent one from the other, the voltage limit for each three-phase voltage space vector is represented by the regular hexagon having the side 2/3 V_{dc}, as depicted in Fig. 3 (dashed line). On the basis of (13), the limit for the six-phase voltage space vector $\overline{v}_{1ref}$ corresponds to the 12-side regular polygon resulting from the intersection of two regular hexagons rotated by 30°, as shown in Fig. 4. In case of sinusoidal balanced voltages, the voltage limit corresponds to the inner circle having radius $V_{dc}/\sqrt{3}$ (shaded area in Fig. 4).

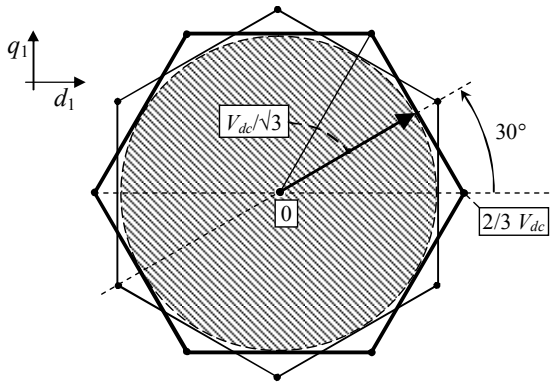

Fig. 4. Voltage limit for sinusoidal balanced voltages.

IV. Dual Three-Phase Induction Machine Model

The behavior of the dual three-phase induction machine having sinusoidal distributed stator windings can be described in terms of multiple space vectors by the following equations, written in a stationary reference frame:

$$\bar{v}_{S1} = R_S \bar{i}_{S1} + \frac{d\bar{\varphi}_{S1}}{dt} \tag{14}$$

$$0 = R_R \bar{i}_{R1} - j p \omega_m \bar{\varphi}_{R1} + \frac{d\bar{\varphi}_{R1}}{dt} \tag{15}$$

$$\bar{\varphi}_{S1} = L_{S1} \bar{i}_{S1} + M_1 \bar{i}_{R1} \tag{16}$$

$$\bar{\varphi}_{R1} = M_1 \bar{i}_{S1} + L_{R1} \bar{i}_{R1} \tag{17}$$

$$\bar{v}_{S5} = R_S \bar{i}_{S5} + \frac{d\bar{\varphi}_{S5}}{dt} \tag{18}$$

$$\bar{\varphi}_{S5} = L_{S\ell} \bar{i}_{S5} \tag{19}$$

$$T = 3 p M_1 \bar{i}_{S1} \cdot j \bar{i}_{R1} . \tag{20}$$

where p is the pole pairs number, ω_m is the rotor angular speed, and the subscripts S and R denote stator and rotor quantities, respectively. It should be noted that $\bar{i}_{S1}$ and $\bar{i}_{R1}$ are responsible for the sinusoidal spatial distribution of the magnetic field in the air gap, whereas $\bar{i}_{S5}$ does not contribute to the air gap field.

V. Simulation Results

In order to verify the effectiveness of the proposed SVM strategy, the behavior of a system consisting of a six-phase VSI feeding a dual three-phase induction motor has been tested by numerical simulations. For the induction motor, the model presented in Section IV has been numerically implemented using the parameters given in Table I, with the rotor speed set to 1430 rpm. The dc bus voltage is $V_{dc} = 310$V.

The choice $\delta_0^{(1)} = \delta_3^{(1)}$ and $\delta_0^{(2)} = \delta_3^{(2)}$ has been considered for the null configurations in each switching period ($T = 200$ μs). The resulting SVM strategy corresponds to the well-known "symmetrical" SVM for each three-phase VSI.

TABLE I
Motor Parameters

P_{rated}	= 4 kW	R_S	= 0.51 Ω
$I_{S,\,rated}$	= 16 A_{rms}	R_R	= 0.42 Ω
$V_{S,rated}$	= 125 V_{rms}	L_{Sl}	= 58.2 mH
ω_S	= 2π50 rad/s	L_{Rl}	= 58.2 mH
p	= 2	M_l	= 56 mH

In the first simulation test, the behavior of the system is analyzed in balanced and sinusoidal conditions, with an amplitude of the reference stator voltage $|\bar{v}_{1ref}|$ = 150 V, frequency 50 Hz, whereas $\bar{v}_{5ref}$ is set to zero. The results are given in Figs. 5-10. In particular, the line-to-neutral voltage waveform v_{S1} (stator phase voltage) is depicted in Fig. 5, showing the characteristic 5-levels waveform of a three-phase VSI. The six stator currents are shown in Fig. 6, and the corresponding harmonic spectrum is shown in Fig. 7. It should be noted that the current waveforms are practically sinusoidal, proving the effectiveness of the proposed SVM strategy, and the current harmonics are concentrated around the frequency of 5 kHz (i.e. the switching frequency).

The trajectories of the space vectors $\bar{i}_{S1}$ and $\bar{i}_{S5}$ in the corresponding d-q planes are shown in Fig. 8, and the corresponding harmonic spectra are shown in Figs. 9 and 10, respectively. As expected, the space vector $\bar{i}_{S5}$ is practically null, apart from the switching ripple (Fig. 10), whereas $\bar{i}_{S1}$ moves along a circular trajectory (at constant speed). The harmonic component at 50 Hz of space vector $\bar{i}_{S1}$ (Fig. 9) corresponds to the harmonic component at 50 Hz of the stator current (Fig. 7).

In the second simulation test, the behavior of the system is analyzed in balanced but non-sinusoidal conditions, with an amplitude of the reference stator voltage $|\bar{v}_{1ref}|$ = 150 V, f_1 = 50 Hz, whereas $|\bar{v}_{5ref}|$ = 15 V, f_5 = 250 Hz (5^{th} harmonic). The results are given in Figs. 11-16. In particular, the stator phase voltage is depicted in Fig. 11, showing a waveform similar to the one of previous case. The six stator currents are shown in Fig. 12, and the corresponding harmonic spectrum is shown in Fig. 13. It should be noted that the currents have the same waveforms, as expected by injecting a 5^{th} harmonic in the second d-q plane (d_5-q_5).

The trajectories of the space vectors $\bar{i}_{S1}$ and $\bar{i}_{S5}$ in the corresponding d-q planes are shown in Fig. 14, and the corresponding harmonic spectra are shown in Figs. 15 and 16, respectively. In this case, both current space vectors $\bar{i}_{S1}$ and $\bar{i}_{S5}$ move along a circular trajectory, at constant speed, apart from the switching ripple. The harmonic component at 50 Hz of space vector $\bar{i}_{S1}$ (Fig. 15) and the harmonic component at 250 Hz of space vector $\bar{i}_{S5}$ (Fig. 16) correspond to the harmonic components of the stator current at 50 Hz and 250 Hz, respectively (Fig. 13).

The simulation tests prove the capability of the proposed SVM technique to generate an arbitrary space vector on both d_1-q_1 and d_5-q_5 planes on the basis of the space vector decomposition expressed by (7).

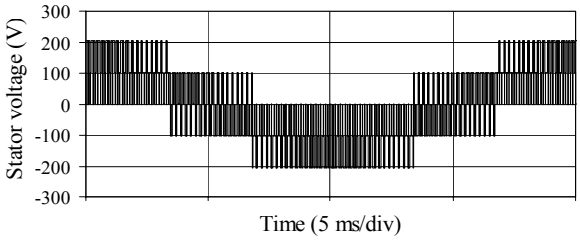

Fig. 5. Stator phase voltage waveform.

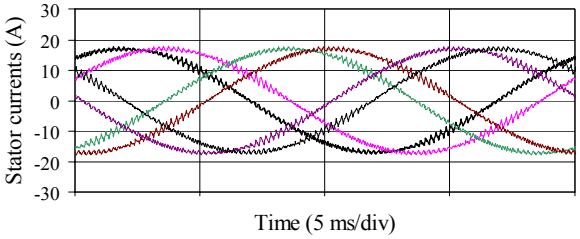

Fig. 6. Stator current voltage waveforms.

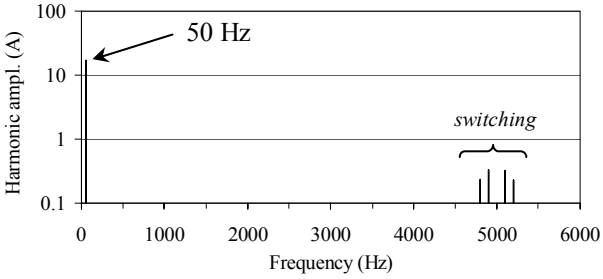

Fig. 7. Harmonic spectrum of the stator current.

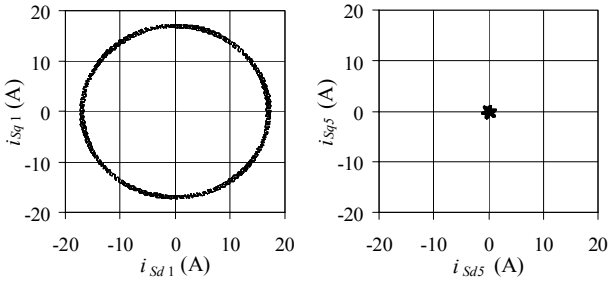

Fig. 8. Trajectories of $\bar{i}_{S1}$ and $\bar{i}_{S5}$ in the corresponding *d-q* planes.

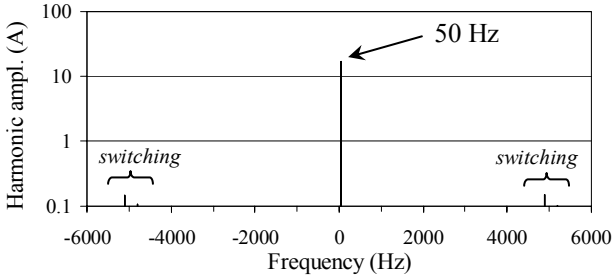

Fig. 9. Harmonic spectrum of space vector $\bar{i}_{S1}$.

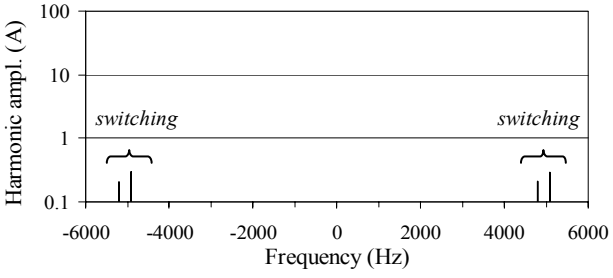

Fig. 10. Harmonic spectrum of space vector $\bar{i}_{S5}$.

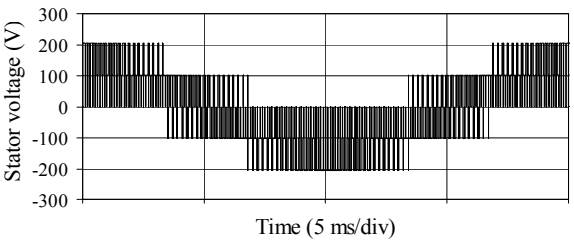

Fig. 11. Stator phase voltage waveform.

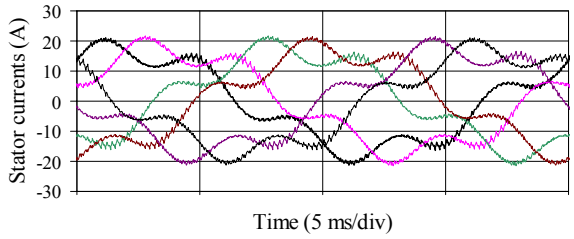

Fig. 12. Stator current voltage waveforms.

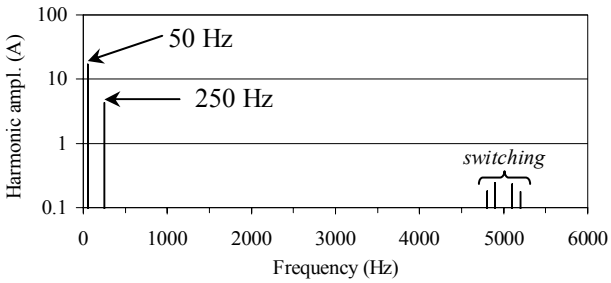

Fig. 13. Harmonic spectrum of the stator current.

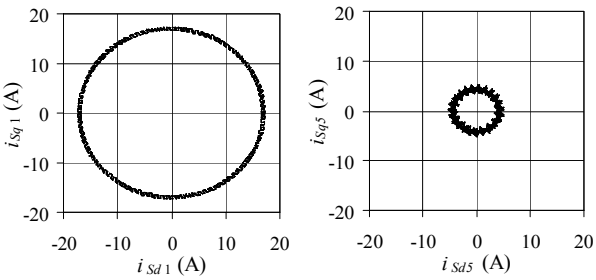

Fig. 14. Trajectories of $\bar{i}_{S1}$ and $\bar{i}_{S5}$ in the corresponding *d-q* planes.

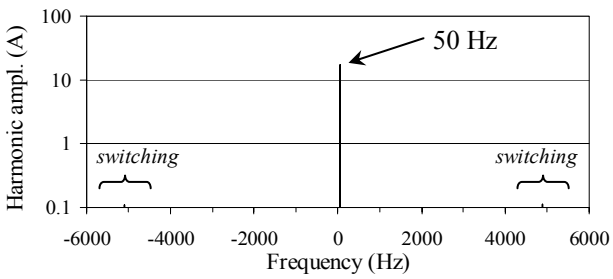

Fig. 15. Harmonic spectrum of space vector $\bar{i}_{S1}$.

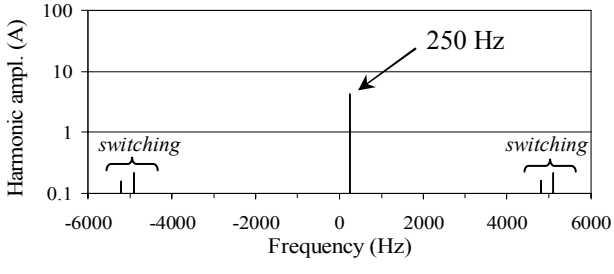

Fig. 16. Harmonic spectrum of space vector $\bar{i}_{S5}$.

VI. Conclusion

A general SVM control strategy for a six-phase VSI based on the concept of three-phase decomposition is presented in this paper. The proposed method allows a full and independent control of the two multiple voltage space vectors of the six-phase VSI in the corresponding *d-q* planes, with an optimal exploitation of the dc input voltage. The modulation limit has been determined with reference to balanced sinusoidal conditions.

The analytical developments have been verified by numerical tests carried out by considering a dual three-phase induction motor load, modeled in terms of multiple space vectors. The numerical results prove the effectiveness of the proposed method.

References

[1] L. Parsa, "On advantages of multi-phase machines," *Proc. of Annual Conference of the IEEE Industrial Electronics Society IECON*, 2005, pp. 1574-1579.

[2] E. Levi, R. Bojoi, F. Profumo, H.A. Toliyat, S. Williamson, "Multi-phase induction motor drives – a technology status review," *IET Electr. Power Appl.*, vol. 1, no.4, pp. 489-516, July 2007.

[3] Y. Zhao, T.A. Lipo, "Space vector PWM control of dual three-phase induction machine using vector space decomposition," *IEEE Trans. on Ind. Applicat.*, vol. 31, no. 5, pp. 1100-1109, September/October 1995.

[4] K.K. Mohapatra, R.S. Kanchan, M.R. Baiju, P.N. Tekwani, K. Gopakumar, "Independent Field-Oriented control of two split-phase induction motors from a single six-phase inverter," *IEEE Trans. on Ind. Electron.*, vol. 52, no. 5, pp. 1372-1382, October 2005.

[5] K. Marouani, L. Baghli, D. Hadiouche, A. Kheloui, A. Rezzoug, "Discontinuous SVPWM techniques for double star induction motor drive control," *Proc. of Annual Conference of the IEEE Industrial Electronics Society, IECON,* November 2006, Hong Kong, pp. 902-907.

[6] D. Hadiouche, L. Baghli, A. Rezzoug, "Space vector PWM techniques for dual three-phase AC machine: analysis, performance evaluation and DSP implementation," *IEEE Trans. on Ind. Applicat.,* vol. 42, no. 4, pp. 1112-1122, July/August 2006.

[7] A.R. Bakhshai, G. Joos, H. Jin, "Space vector PWM control of a split-phase induction machine using the vector classification technique," *Proc. of IEEE Applied Power Electronics Conference and Exposition, APEC*, 15-19 February 1998, Hong Kong, pp. 802-808.

[8] D. Yazdani, S.A. Khajehoddin, A. Bakhshai, G. Joos, "A generalized space vector classification technique for six-phase inverters," *Proc. of IEEE Power Electronics Specialist Conference, PESC*, 17-21 June 2007, Hong Kong, pp. 2050-2054.

[9] R. Bojoi, A. Tenconi, F. Profumo, G. Griva, D. Martinello, "Complete analysis and comparative study of digital modulation techniques for dual three-phase AC motor drives," *Proc. of IEEE Power Electronics Specialist Conference, PESC*, 23-27 June 2002, Hong Kong, pp. 851-857.

[10] G. Grandi, G. Serra, A. Tani, "Space vector modulation of nine-phase voltage source inverters based on three-phase decomposition," 12th European Conference on Power Electronics and Applications, EPE 2007, Aalborg (DK), September 2-5, 2007.